Transp Porous Med
DOI 10.1007/s11242-011-9752-7

Capillary Pressure Curve for Liquid Menisci in a Cubic Assembly of Spherical Particles Below Irreducible Saturation

Jacob Bear · Boris Rubinstein · Leonid Fel

Received: 6 October 2010 / Accepted: 2 March 2011

Abstract The capillary pressure–saturation relationship, $P_c(S_w)$, is an essential element in modeling two-phase flow in porous media (PM). In most practical cases of interest, this relationship, for a given PM, is obtained experimentally, due to the irregular shape of the void space. We present the $P_c(S_w)$ curve obtained by basic considerations, albeit for a particular class of regular PM. We analyze the characteristics of the various segments of the capillary pressure curve. The main features are the behavior of the $P_c(S_w)$ curve as the wetting-fluid saturation approaches zero, and as this saturation is increased beyond a certain critical value. We show that under certain conditions (contact angle, distance between spheres, and saturation), the value of the capillary pressure may change sign.

Keywords Porous media · Two-phase flow · Wetting fluid · Capillary pressure curve

List of Symbols

d	Distance between spheres
n	Number of spheres per unit cell
H	Mean curvature of meniscus
P_c	Capillary pressure
P_w, P_n	Pressures in wetting and non-wetting fluids
R	Radius of sphere
S_w, S_n	Saturations of wetting and non-wetting fluids
S_{wr}, S_{nr}	Irreducible w-fluid and residual n-fluid saturations

This article is dedicated to the memory of Prof. Walter Rose (1920–2009), a friend, engineer and scientist, who did pioneering work on the capillary pressure curve in reservoir engineering.

J. Bear (✉) · L. Fel
Department of Civil Engineering, Technion, 32000 Haifa, Israel
e-mail: cvrbear@techunix.technion.ac.il

B. Rubinstein
Stowers Institute for Medical Research, Kansas City, MO 64110, USA

Published online: 30 March 2011

V Volume of pendular ring
γ Surface tension of the w–n interface
θ Contact angle
ϕ Porosity
ψ Filling angle

1 Introduction

Porous medium (PM) domains can be divided into two major groups with respect to the characteristic dimensions of the void space. Those in which the void space can be visualized as a network of "pores" and "channels," and those composed of a network of fractures. The main difference between these two groups is that while all three dimensions of a "pore" are almost the same, a channel has two dimensions that are smaller than the third one, and a fracture has one dimension smaller than the other two. In this article, we focus on PMs belonging to the first group.

An essential concept in two-phase flow in PM is the *capillary pressure relationship*. It is a consequence of the *interfacial tension*, γ, that acts within the interface separating two fluid phases—a *wetting* (w) and a *non-wetting* (n)—that together occupy the entire void space at *saturations* S_{w} and $S_{\mathrm{n}}(= 1 - S_{\mathrm{w}})$. At any point on the w–n interface, the difference between the pressures on the corresponding sides of the latter is called *capillary pressure*, P_{c}. It is given by the Young–Laplace formula,

$$P_{\mathrm{c}} \equiv P_{\mathrm{n}} - P_{\mathrm{w}} = 2\gamma H(S, \theta)\cos\theta, \quad H = \frac{1}{2}\left(\frac{1}{R_1} + \frac{1}{R_2}\right), \tag{1}$$

in which R_1, R_2 denote the *principal radii of curvature*, H denotes the *mean curvature* of the interface, and θ denotes the *contact angle* corresponding to the considered solid and two fluids, the w- and n-fluids. The Young–Laplace equation is a necessary requirement that ensures that shape of the fluid–fluid interface corresponds to the state of minimum surface energy. In the work presented here, we have neglected the w-fluid–solid interaction, as well as the presence of a film on the solid. The surface tension between the w-fluid and the solid, between the n-fluid and the solid and between the two fluids is represented by the contact angle (Young relation).

Figure 1 shows two typical $P_{\mathrm{c}}(S_{\mathrm{w}})$ curves. The blue curve is a typical *drainage curve*, i.e., drainage of the w-fluid, starting from a void space that is occupied only by the w-fluid, at $S_{\mathrm{w}} = 1.0$. As this fluid is being drained, with the larger pores being drained first, the n-fluid invades these pores. The P_{c} rises due to the increase in H (i.e., smaller menisci) as the w-fluid remains in smaller pores. We follow the *drainage curve*, until, at some S_{w}, the w-fluid becomes discontinuous, and flow/drainage cannot take place. This value, $S_{\mathrm{w}} = S_{\mathrm{wr}}$, is called *irreducible w-fluid saturation*. If, starting at $S_{\mathrm{w}} = S_{\mathrm{wr}}$ we reverse the process, i.e., the n-fluid is drained out and the w-fluid gradually fills-up the void space, P_{c} decreases. This is shown as the black curve. When the saturation of the n-fluid reaches the point at which this fluid becomes discontinuous, at *residual* n-*fluid saturation*, $S_{\mathrm{n}} = S_{\mathrm{nr}}$, no further drainage of the n-fluid is possible. The phenomenon manifested by the two different curves—for drainage and for imbibition—is called *hysteresis*.

These two curves, obtained *experimentally*, are used in two-phase flow in PM, e.g., in petroleum engineering and in soil-physics, where the n-fluid is air.

Actually, the term "irreducible w-fluid saturation," introduced by soil physicists in the 30's, is inappropriate, as the saturation can further be reduced by evaporation (e.g., Bear

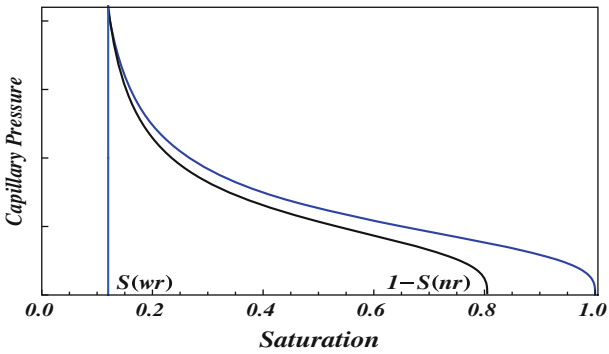

Fig. 1 Typical capillary pressure curves, $P_c = P_c(S_w)$, showing a drainage curve (*blue*) and an imbibition curve (*black*)

and Cheng 2010). Furthermore, if we start from a completely dry sample, i.e., $S_w = 0$, and produce condensation, say of a w-fluid vapor present in the n-fluid, we can trace a wetting curve as S_w increases, covering the range $0 < S_w < S_{wr}$. What is actually meant by this term is that below this saturation, a reduction produced by flow of the wetting fluid is not possible, because the w-fluid is discontinuous. However, the fact that the wetting phase is discontinuous does not mean that a further reduction in saturation is not possible. Nevertheless, following tradition, we shall continue to refer here to "irreducible w-fluid saturation." Changes in saturation in this range will be due to condensation and evaporation, or to changes of concentration of a dissolved gas in a liquid–gas system.

Brooks and Corey (1964), Van Genuchten (1980), Rossi and Nimmo (1994), and others suggested formulae for $P_c(S_w)$, obtained by curve-fitting to experiments, with coefficients that have to be adjusted for particular PMs. Typically, these experiments involve drainage and imbibition of the w-fluid. However, these formulae, e.g., van Genuchten's, lead to an infinite P_c-value at $S_w = S_{wr}$. In practice, the P_c-value does not reach infinity. Instead, the curve should terminate at some finite value that corresponds to the saturation S_{wr} at which the w-fluid becomes discontinuous. Because S_w may further be reduced by evaporation, the capillary pressure curve should be extended to the range $S_w < S_{wr}$. To our best knowledge, the capillary pressure curve in this range has not been investigated.

Regarding theoretical works, there have been very few attempts to obtain the capillary pressure–saturation relationship by analyzing simplified PM models. (Collins, 1961, p. 25) represented the solid matrix as an assembly of parallel circular rods in a square packing and studied the 2-dim pendular rings between them. Rose (1958) studied $P_c(S_w)$ by representing the solid matrix as an assembly of spheres in a 3-dim *simple cubic packing*, assuming that the pendular ring between adjacent spheres is bounded by a surface of revolution (meniscus) of a *circular meridian curve*. Both have covered only the range of saturation corresponding to *disjoint menisci*. Gwirtzman and Roberts (1991) studied pendular rings and ganglia when two-phases occupy the void space produced by various arrangements of spheres. However, the menisci in the models used in the last two references do not satisfy the Young equation.

In this conjunction, two papers, by Melrose (1966) and Orr et al. (1975), are of high relevance. They develop, for the first time, an explicit solution of the Young–Laplace equation for the shape of the meniscus bounding the pendular ring between two equal solid spheres.

Melrose (1966) and Orr et al. (1975) expressed H by

$$2H = \frac{\mathrm{d}^2 z/\mathrm{d}r^2}{[1 + (\mathrm{d}z/\mathrm{d}r)^2]^{3/2}} + \frac{\mathrm{d}z/\mathrm{d}r}{r[1 + (\mathrm{d}z/\mathrm{d}r)^2]^{1/2}}, \tag{2}$$

in which the shape of the axisymmetric meniscus is given by $z = z(r)$.

In another approach (Or and Tuller 1999; Patzek 2001), based on statistics, the void space is represented as a network of "boxes," or "pore bodies," connected by narrow "channels," "pore-throats," or "ducts," with various cross-sections (circular, triangular, and square). By making certain assumptions with respect to the evolution of the w–n interface in the corners of the "pore throats" and the statistics of pore sizes, they obtain a $P_c(S_w)$-curve. In these models, there is no reference to the concept of irreducible w-fluid saturation.

However, although *flow* cannot occur in the range $S_w \leq S_{wr}$, the $P_c(S_w)$-relationship in this range does play an important role when we deal with evaporation and condensation phenomena, e.g., in drying. Furthermore, it is important to understand the nature of the relationship $P_c(S_w)$ in this range in order to investigate it for $S_w > S_{wr}$.

In this article, our objective is to focus on the part of the capillary pressure curve, $P_c(S_w)$, in the range $0 < S_w < S_{wr}$, making use of a *geometrical approach* that is based on the Young–Laplace equation (1), and employing a PM made up of ordered spheres arranged as *periodic unit cells*. Then, we show certain specific features of the $P_c(S_w)$-curve that have hitherto not been mentioned in the literature. Four assumptions underlie our discussion: (a) gravity is neglected, (b) we neglect the presence of a w-film on the solid, (c) the contact angle, θ, undergoes no hysteresis, and (d) the surface tension is assumed constant. Because we are considering saturations only in the range in which the menisci are not connected, and, hence, flow cannot occur, changes in saturation are due only to condensation and evaporation of the w-fluid, or changes in the concentration of a gas dissolved in a liquid.

2 Pendular Ring of Constant Mean Curvature (CMC)

The *Plateau sequence* (Plateau 1864) describes the shapes of the pendular rings between a w- and n-fluids produced in the vicinity of the contact between two identical touching spheres. At a small volume of the w-fluid, the pendular ring takes the shape of a surface of revolution produced by a *negative nodoid* as a generating curve, with $H < 0$. As the volume of the w-fluid increases, this shape undergoes a sequence of changes, leading to a surface generated by a *positive nodoid* with $H > 0$. This sequence is shown schematically as:

$$\begin{array}{ccccccc}
\boxed{Negative\ Nodoid} & \Rightarrow & \boxed{Catenoid} & \Rightarrow & \boxed{Negative\ Unduloid} & \Rightarrow & \boxed{Cylinder} \\
R_1 > 0,\ R_2 < 0 & & R_1 > 0,\ R_2 < 0 & & R_1 > 0,\ R_2 < 0 & & R_1 > 0,\ R_2 = \infty \\
H < 0,\ G < 0 & & H = 0,\ G < 0 & & H > 0,\ G < 0 & & H > 0,\ G = 0
\end{array}$$

$$\Longrightarrow \boxed{Positive\ Unduloid} \Rightarrow \boxed{Sphere} \Rightarrow \boxed{Positive\ Nodoid} \tag{3}$$

$$R_1 > R_2 > 0 \qquad R_1 = R_2 > 0 \qquad R_2 > R_1 > 0$$
$$H > 0,\ G > 0 \qquad H > 0,\ G > 0 \qquad H > 0,\ G > 0$$

In each case, we have indicated also the mean curvature, H, and the *Gauss curvature* $G = R_1^{-1} R_2^{-1}$, defined by the principal radii of curvature. The *filling angle*, ψ, is shown in Fig. 2. When $\theta = 0$, the last shape in the above sequence is the *positive unduloid*.

In this article, we consider the simple case of two touching identical spheres. The dependence of the mean curvature, H, on the volume of the pendular ring, V, for a given θ, was

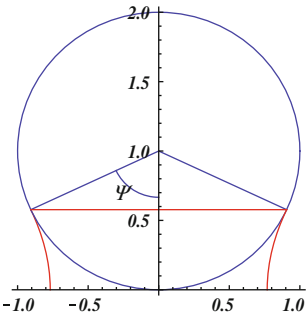

Fig. 2 The upper half of a negative unduloid (*in red*), for $\theta = 0°$, $\psi = 65°$

presented by Melrose (1966) and Orr et al. (1975). In the case of a negative nodoid (n), H and V satisfy the two non-linear equations:

$$2H_{\mathrm{n}}R = A(\psi)\left\{B(\psi,\theta) - \frac{1}{k}\mathcal{E}(\psi,\theta,k) + \frac{1-k^2}{k}\mathcal{F}(\psi,\theta,k)\right\}, \tag{4}$$

$$V_{\mathrm{n}} = \frac{\pi}{8H_{\mathrm{n}}^3}\left(\mu+\nu+\frac{k}{3}c(c+4)\mathcal{F}(\psi,\theta,k) - \frac{k}{3}(c+1)(c+8)\mathcal{E}(\psi,\theta,k)\right) - \pi\left(\frac{2}{3} - \cos\psi + \frac{1}{3}\cos^3\psi\right), \tag{5}$$

where R is the radius of a sphere, and $A(\psi) = \frac{1}{1-\cos\psi}$, $B(\psi,\theta) = -\cos(\psi-\theta)$, $c = 4H_{\mathrm{n}}R\sin\psi\,[H_{\mathrm{n}}R\sin\psi - \sin(\theta+\psi)]$, $k = \frac{1}{\sqrt{1+c}}$, $\mu = \frac{4}{3}\cos^3(\psi+\theta) - (c+4)\cos(\psi+\theta)$, $\nu = \frac{2}{3}\sin 2(\psi+\theta)\sqrt{\sin^2(\psi+\theta)+c}$, and

$$\mathcal{E}(\psi,\theta,k) = E\left(\frac{\pi}{2},k\right) - E\left(\frac{\pi}{2}-\psi-\theta,k\right),$$
$$\mathcal{F}(\psi,\theta,k) = F\left(\frac{\pi}{2},k\right) - F\left(\frac{\pi}{2}-\psi-\theta,k\right),$$

where $F(\phi,k)$ and $E(\phi,k)$ are elliptic integrals of the 1st and 2nd kinds, respectively. Analogous equations can be written for non-touching spheres; they are not shown here because they are much more cumbersome and lengthy.

In Fig. 3, we present the relationship $H(\psi)$ for two pendular rings, between two *touching* spheres, with $\theta = 0$ and $\theta = \pi/6$. It shows a continuous behavior in the entire range $0 \le \psi \le \pi$ and indicates the critical value ψ_{c}, where the curvature of the meniscus changes its sign, and the *catenoidal* shape arises.

In the general case of non-touching spheres, our numerical solution of equations that are analogous to (4) and (5), obtained by using the computer algebra software *Mathematica*, shows that the Plateau sequence of the menisci shapes, presented as (3), has to be prepended (to the left in (3)) by negative unduloid.

Figure 4 shows a variety of shapes that the dependence $H(\psi)$ can take on when the two identical spheres are at a distance d. We note that, contrary to what we see in Fig. 3, the green line in Fig. 4 corresponds to a $H > 0$ for the *entire* range of ψ, recalling that ψ is related to the saturation. In fact, the green line resembles the conventional $H(S_{\mathrm{w}})$-relationship. However, the other curves are interesting, as they indicate that under certain conditions on ψ and d, i.e., conditions of saturation, the relationship $H(\psi)$ exhibits changes in mean curvature sign. Since H is related to $P_{\mathrm{c}}(S_{\mathrm{w}})$ through the Laplace–Young formula, this imposes a change of sign of P_{c}. There is no support in the literature to this conclusion as all retention curves

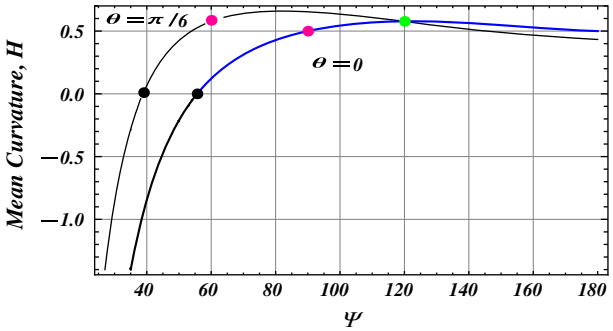

Fig. 3 Plots of $H(\psi)$ for two menisci, with $\theta = 0$ and $\theta = \pi/6$. The values of ψ_c, where the *catenoidal* shapes appear ($H = 0$), are $\psi_c(\theta = 0°) = 55.4°$ and $\psi_c\left(\theta = 30°\right) = 39°$; they are indicated as *black* points. The *nodoidal* and *unduloidal* shapes of menisci are drawn in *black* and *blue* colors, respectively. The *red* points mark the menisci having the shape of a cylinder, while the *green* point stands for the meniscus with a spherical shape

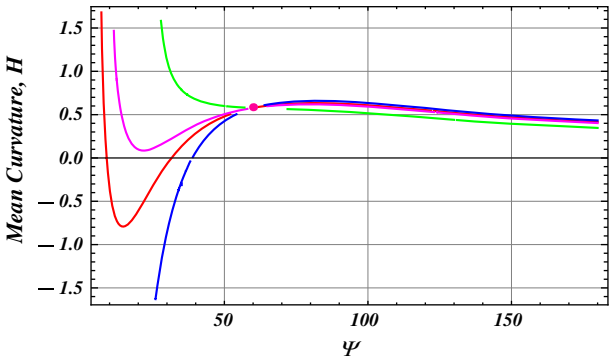

Fig. 4 Plots of $H(\psi)$ for menisci with $\theta = \pi/6$ and different distances, d, between two solid spheres: $d = 0$ (*blue*), $d = 0.18R$ (*red*), $d = 0.3R$ (*pink*), and $d = R$ (*green*)

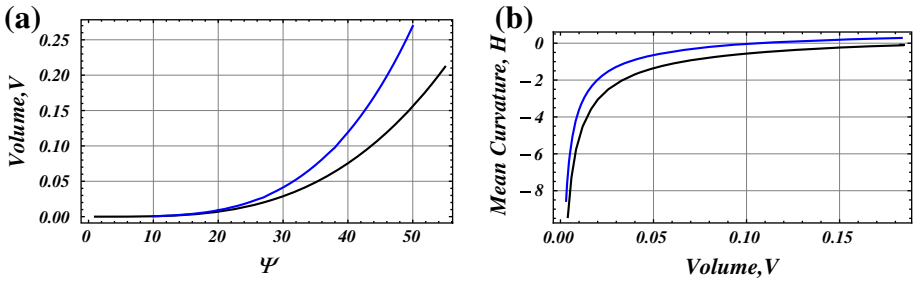

Fig. 5 Plot of $V(\psi)$ (**a**) and $H(V)$ (**b**) for menisci with $\theta = 0°$ (*black*) and $\theta = 30°$ (*blue*)

are presented for $S_w > S_{wr}$. However, Nitao and Bear (1996) do show that $P_c(S_w)$ can take on negative values. In Fig. 5, we present typical dependences $V(\psi)$ and $H(V)$ for liquid pendular rings of the *nodoidal* shape.

Other important characteristics of the meniscus are the asymptotic behavior of its curvature, $H \simeq \psi^{\kappa}$ and its volume $V \simeq \psi^{\epsilon}$, as $\psi \to 0$. In the case $\theta = 0$, an exact analysis shows

that

$$\kappa = -2\,, \quad \epsilon = 4, \qquad \text{such that} \quad H \simeq V^{-\delta}, \quad \delta = \frac{1}{2}\,. \tag{6}$$

This δ value is *exact* and coincides with a similar exponent of an approximate model of the meniscus when its shape is often considered as part of a *toroidal* surface.

It can be shown (K. Brakke, Susquehanna Univ., PA, private communication) that for contact angles $\theta < 30°$, the shape of the *negative nodoidal* meniscus is stable under small perturbations.

3 The Porous Medium Models

We consider two PM models as repetitive unit cells, each composed of an assembly of touching rigid spheres. Such structures exhibit all the relevant features of a PM, while enabling the analysis of the shape of the interface between two immiscible fluids, w and n, which jointly occupy the entire void space. Two different unit cubic cells, *simple cubic*, SC, and *body center cubic*, BCC, are presented in Fig. 6. Table 1 presents a number of relevant characteristic properties of these two structures: R = radius of sphere, ϕ = porosity, n = number of spheres per cell, and ρ = radius of the largest sphere that can be inscribed in the void space. One additional important characteristic is the angle, β, between two radius vectors, which connect the center of a sphere with the centers of the two closest adjacent spheres that touch the former. For both models, we choose the contact angles $\theta = 0$ and $\theta = 30°$.

Figure 6 shows how the SC and BCC unit cells look like when their void space is partially occupied by the w-fluid producing disjoined pendular rings

4 Capillary Pressure for $S_w \leq S_{wr}$

In this range, all pendular rings are identical and disconnected. The value of S_{wr} can be found separately for the SC and BCC structures. It is easy to show that two adjacent pendular

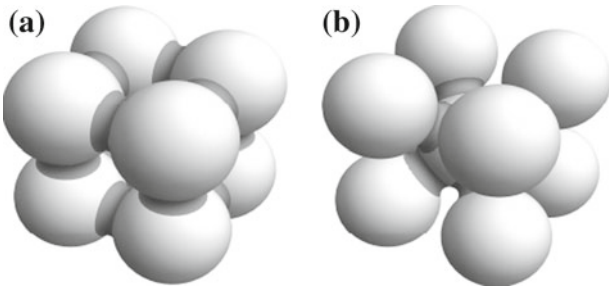

Fig. 6 Unit cells of the SC (**a**) and BCC (**b**) arrangements of the touching solid spheres

Table 1 Characteristic properties of the SC and BCC structures

	R	ϕ	n	β	ρ
SC	0.5	0.476	1	90°	0.366
BCC	0.433	0.320	2	70.53°	0.097

rings meet each other on the solid surface when the filling angle, ψ, will reach its value $\beta/2$ (see Table 1). For the two structures considered here, this gives: $\psi_{\rm wr}(SC) = 45°$ and $\psi_{\rm wr}(BCC) = 35.26°$. Figure 7a and b illustrates the moment when liquid pendular rings begin to touch each other. The saturation $S_{\rm wr}$ depends on $\psi_{\rm wr}$ via the total volume of pendular rings which occupy part of the void space inside the unit cell. For $\theta = 0°$ one obtains

$$\begin{aligned} S_{\rm wr}(SC) &= 3R_{SC}^3 \cdot \frac{V_{SC}(45°)}{\phi_{SC}} \simeq 0.1733, \\ S_{\rm wr}(BCC) &= 8R_{BCC}^3 \frac{V_{BCC}(35.26°)}{\phi_{BCC}} \simeq 0.0761. \end{aligned} \tag{7}$$

For $\theta = 30°$, the corresponding values are $S_{\rm wr}(SC) = 0.288$ and $S_{\rm wr}(BCC) = 0.114$.

When $S < S_{\rm wr}$, the liquid pendular rings are disconnected. What is also important is that for $\theta = 0$ and $\psi_{\rm c}(0°) \simeq 55.4°$, we have,

$$\psi_{\rm wr}(SC) < \psi_{\rm c}(0°)\ , \quad \psi_{\rm wr}(BCC) < \psi_{\rm c}(0°)\ , \tag{8}$$

i.e., the mean curvature H of the liquid menisci in both structures does not change its sign when the saturation $S_{\rm w}$ increases in the range $(0, S_{\rm wr})$.

However, when θ increases one can easily find a structure where (8) does not hold. Indeed,

$$\begin{aligned} &\theta = 30°,\ \psi_{\rm c}(30°) \simeq 39° \ : \quad \psi_1(SC) > \psi_{\rm c}(30°)\ , \quad \psi_1(BCC) < \psi_{\rm c}(30°), \\ &\theta = 60°,\ \psi_{\rm c}(60°) \simeq 20° \ : \quad \psi_1(SC) > \psi_{\rm c}(60°)\ , \quad \psi_1(BCC) > \psi_{\rm c}(60°)\ . \end{aligned} \tag{9}$$

Figure 8 shows the relationship between the capillary pressure and saturation. However, here, as is commonly done in reservoir engineering, we express the capillary pressure as a modified Leverett function, $J(S_{\rm w})$

$$J(S_{\rm w}) = \frac{P_{\rm c}(S_{\rm w})R}{\gamma}, \quad S_{\rm w} = \frac{3V_{\rm menis}}{1 - (\pi/6)(1 + d/R)^3}, \tag{10}$$

in which the radius of the sphere, R, represents the characteristic length of the considered void space. Note that the curves in Fig. 8 end at the value $S_{\rm wr}$ that corresponds to the associated distance d. Similar curves can be shown for the BCC structure.

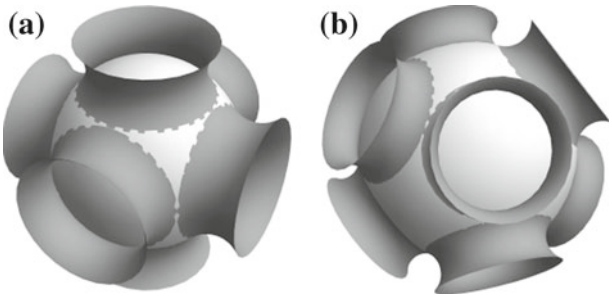

Fig. 7 The solid sphere with **a** six liquid pendular rings (SC) and **b** eight liquid pendular rings (BCC), at the moment when they begin to touch each other

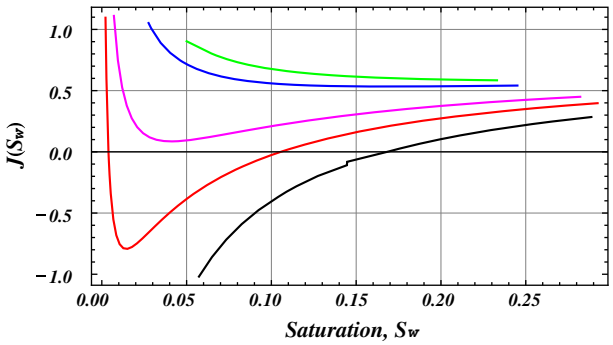

Fig. 8 Plots of capillary pressure curve $J(S_{\rm w})$ for menisci in an SC structure, with $\theta = \pi/6$ and different distances, $d(\geq 0)$, between two solid spheres: $d = 0$ (*black*), $d = 0.18R$ (*red*), $d = 0.3R$ (*pink*), $d = 0.6R$ (*blue*), and $d = 0.8R$ (*green*)

5 Concluding Remarks and Discussion

In this section, we summarize the developments on the $P_{\rm c}(S_{\rm w})$-curve in the range below the irreducible w-fluid saturation, $S_{\rm wr}$. Beyond this value, the physics becomes more interesting (e.g., the wetting phase becomes interconnected and flow is possible), but the necessary mathematical tools are more complicated. Thus, we suggest certain directions for further research required to construct the $P_{\rm c}(S_{\rm w})$-curve for the entire range of saturations.

1. The capillary pressure curve in the range $S_{\rm w} < S_{\rm wr}$, in which the wetting fluid takes the form of disjoined pendular rings so that changes in $S_{\rm w}$ can be produced only by evaporation and condensation, was obtained for the SC and BCC 3D arrangements of equal solid spheres, by solving the Young–Laplace equation. The solutions depend on a finite number of relevant geometrical parameters: the contact angle, θ, the relative distance between the spheres, d/R, the type of the repetitive structure, e.g., SC or BCC, and the physical parameter, γ (=surface tension). The latter serves as a scaling parameter.
2. The value of $S_{\rm wr}$, commonly referred to as "irreducible w-fluid saturation" was calculated; it also depends on θ, d/R and the type of structure. The capillary pressure curve in this range of $S_{\rm w}$ is seldom mentioned in the literature.
3. We show that in the range $0 \leq S_{\rm w} \leq S_{\rm wr}$, the value of the capillary pressure can take *negative* values. It can also change sign more than once. So far, such behavior has not been reported in the literature, although such possibility has been occasionally indicated.
4. The sign change of $P_{\rm c}$ as $S_{\rm w}$ varies cannot be reached in models where the meniscus bounding the pendular ring is approximated by a toroidal surface (i.e., a surface of revolution generated by a circle rotating around an axis of symmetry). When a meniscus is concave or convex (like when a fluid rises or drops in a capillary tube, depending in whether the fluid is wetting or non-wetting with respect to the tube), it is obvious that the meniscus is either concave or convex. However, between the two non-touching spheres considered here, we have shown that the meniscus may take on the form of a "saddle," such that we have surfaces with radii of curvature which are both positive and negative, and there is an interplay between their magnitudes. This leads to a curvature, H, which is sometime negative and in other cases positive. If we maintain the n-fluid at a constant pressure, then the pressure in the w-fluid may be positive or negative (with respect to the pressure in the n-fluid).

5. Although we have been discussing PM models composed of spheres, the above conclusions remain valid also for non-spherical (but convex) granules.
6. The derivation of the $P_c(S_w)$ relationship in the range $S_w < S_{wr}$ should be of interest to those dealing with wetting and drying of granular materials. We recall that according to Kelvin's law, the capillary pressure is related to the relative humidity of the air (in an air–water system). Appropriate instrumentation, based on evaporation and condensation, has to be developed in order to verify the relationships derived here.

Although this article focuses on the $P_c(S_w)$-relationship ($\equiv P_n - P_w$) in the range $S_w < S_{wr}$, a few observations and comments may be added on this relationship in the range $S_w > S_{wr}$. We recall that the curve is shown as a P_c-curve, but, with an appropriate scaling, actually, it describes the relationship $H(S_w)$. Let us continue to make the assumption of no gravity.

6 A Few Observations on the Range $1 - S_{nr} < S_w < 1.0$

The curve $P_c(S_w)$, found in the literature, especially in soil physics, is, usually, shown as composed of two parts: the first part is obtained when a fully saturated sample ($S_w = 1$) is drained, until drainage stops (or practically so), with cessation of drainage occurring when the w-fluid becomes discontinuous (i.e., zero effective permeability). The other part occurs when the flow direction is reversed, with the w-fluid gradually invading the sample by *imbibition*. However, this process is terminated when, at some saturation, called residual n-fluid saturation ($= 1 - S_{nr}$), the n-fluid becomes discontinuous (i.e., zero effective permeability). Thus, the shape of the curves reflects the method (e.g., based on flow) used for their determination. We have devoted this article to the discussion of what happens in the range $S_w < S_{wr}$. What happens in the range $1 - S_{nr} < S_w \leq 1$?

In fact, suppose we stop imbibition at some S_w-value, which is slightly less than $S_w = 1 - S_{nr}$. Both fluids are continuous and we get a point on the $P_c(S_w)$-curve. If we further increase S_w, at some point the n-fluid becomes *discontinuous*. What is then the P_c at this point? It is equal to the pressure jump across the interface bounding the occluded *ganglia*. Can we measure the pressure inside the ganglia? The entrapped n-fluid is immobile. Can we reach $H = 0$? or $P_c = 0$ ($\equiv P_w = P_n$)?

Let us now start from $S_w = 1$, and assume that the w-fluid contains a dissolved gas or dissolved n-fluid. By changing conditions, e.g., temperature, part of the dissolved n-fluid comes out of solution and forms a large number of tiny bubbles, which eventually coalesce (no gravity!) to a single spherical bubble in each portion of the void space. By controlling dissolution, this bubble grows until it touches the solid surface. The spherical bubble has a constant radius, i.e., constant H. As long as this bubble can grow, H decreases, and with it also P_c. Altogether, this means that *in principle* the $P_c(S_w)$ curve should also exist to the right of $S_w = 1 - S_{nr}$, and that we need to develop appropriate instrumentation to obtain this part of the $P_c(S_w)$-curve.

We wish to reiterate that the objective of this work was to investigate the capillary pressure curve, primarily in the range below the irreducible w-fluid saturation, theoretically. To achieve this goal, we have made certain simplifying assumptions, e.g., the PM is made up of a periodic distribution of spheres of uniform size, constant contact angle, constant surface tension, and the absence of films on the solid surface. A real PM is much more complicated, e.g., a grain-size distribution, non-uniform sphere sizes, a random arrangement of grains in space, variable contact angle, and surface tension, also as water evaporates and air dissolves in water. However, we believe that our selected set of assumptions does represent the major

features of the investigated phenomena. Obviously, what is required now is experimental work to validate our model and to determine the capillary pressure curves for particular porous media.

Acknowledgment The useful discussions with K. Brakke on stability of the shape of menisci below and above the irreducible saturation are appreciated. This research was supported partly by funds from the European Community's Seventh Framework Programme FP7/2007-2013 under grant agreement no. 227286 as part of the MUSTANG project, and partly by the Kamea Fellowship program.

References

Bear, J., Cheng, A.H.-D: Modeling Groundwater Flow and Contaminant Transport. Springer, Berlin (2010)

Brooks, R.J., Corey, A.T.: Hydraulic properties of porous media. Hydrology Paper 3, Colorado State University, Fort Collins (1964)

Collins, R.E.: Flow of Fluids Through Porous Materials. Reinhold Publishing Corp, New York (1961)

Gwirtzman, H., Roberts, P.V.: Pore scale spatial analysis of two immiscible fluids. Water Resour. Res. **27**(6), 1165–1176 (1991)

Melrose, J.C.: Model calculations for capillary condensation. AIChE J. **12**(5), 986–994 (1966)

Nitao, J.J., Bear, J.: Potentials and their role in transport in porous media. Water Resour. Res. **32**(2), 225–250 (1996)

Or, D., Tuller, M.: Liquid retention and interfacial area in variably saturated porous media: upscaling from single-pore to sample-scale model. Water Resour. Res. **35**(12), 3591–3600 (1999)

Orr, F.M., Scriven, L.E., Rivas, A.P.: Pendular rings between solids: meniscus properties and capillary force. J. Fluid Mech. **67**(4), 723–742 (1975)

Patzek, T.: Verification of a complete pore network simulator of drainage and imbibition. Soc. Petrol. Eng. **71310**, 144–156 (2001)

Plateau, J.: The figures of equilibrium of a liquid mass, pp. 338–369. The Annual Report of the Smithsonian Institution, Washington, DC (1864)

Ramirez-Flores, J.C., Bachmann, J., Marmur, A.: Direct determination of contact angles of model soils in comparison with wettability characterization by capillary rise. J. Hydrol. (2010)

Rose, W.: Volume and surface areas of pendular rings. J. Appl. Phys. **29**(4), 687–691 (1958)

Rossi, C., Nimmo, J.R.: Modeling of water retention from saturation to oven dryness. Water Resour. Res. **30**(3), 701–780 (1994)

van Genuchten, M.T.: A closed-form equation for predicting the hydraulic conductivity of unsaturated soils. Soil Sci. Soc. Am. **44**, 892–898 (1980)